Published in final edited form as:
Circulation. 2016 September 13; 134(11): 817–832. doi:10.1161/CIRCULATIONAHA.115.016423.

Glycoproteomics Reveals Decorin Peptides with Anti-Myostatin Activity in Human Atrial Fibrillation

Javier Barallobre-Barreiro, PhD[1], **Shashi K. Gupta, PhD**[2], **Anna Zoccarato, PhD**[1], **Rika Kitazume-Taneike, MD**[1], **Marika Fava, MSc**[1,3], **Xiaoke Yin, PhD**[1], **Tessa Werner, MSc**[4], **Marc N Hirt, MD, PhD**[4], **Anna Zampetaki, PhD**[1], **Alessandro Viviano, MD**[3], **Mei Chong, PhD**[1], **Marshall Bern, PhD**[5], **Antonios Kourliouros, MD**[3], **Nieves Domenech, PhD**[6], **Peter Willeit, MD, PhD**[1], **Ajay M Shah, MD**[1], **Marjan Jahangiri, MD**[3], **Liliana Schaefer, MD**[7], **Jens W. Fischer, PhD**[8], **Renato V. Iozzo, MD**[9], **Rosa Viner, PhD**[10], **Thomas Thum, MD, PhD**[2], **Joerg Heineke, MD**[11], **Antoine Kichler, PhD**[12], **Kinya Otsu, MD, PhD**[1], and **Manuel Mayr, MD, PhD**[1]

[1]King's British Heart Foundation Centre, King's College London, London, UK

[2]Institute for Molecular and Translational Therapeutic Strategies, MH-Hannover, Germany

[3]St George's Hospital, NHS Trust, London, UK

[4]University Medical Center Hamburg-Eppendorf, Hamburg, Germany

[5]Protein Metrics, San Carlos, USA

[6]Biobanco A Coruña, INIBIC-Complexo Hospitalario Universitario de A Coruña, Spain

[7]Klinikum der Goethe-Universität, Frankfurt am Main, Germany

[8]Institute for Pharmacology and Clinical Pharmacology, Heinrich-Heine-University, Düsseldorf, Germany

[9]Sidney Kimmel Medical College at Thomas Jefferson University, Philadelphia, USA

[10]Thermo Fisher Scientific, San Jose, USA

[11]Experimental Cardiology, Department of Cardiology and Angiology, MH-Hannover, Germany

[12]Laboratoire Vecteurs: Synthèse et Applications Thérapeutiques, UMR 7199 CNRS Université de Strasbourg, Illkirch, France

Abstract

Background—Myocardial fibrosis is a feature of many cardiac diseases. We used proteomics to profile glycoproteins in the human cardiac extracellular matrix (ECM).

Methods—Atrial specimens were analyzed by mass spectrometry after extraction of ECM proteins and enrichment for glycoproteins or glycopeptides.

Address for Correspondence: Manuel Mayr, MD, PhD, King's British Heart Foundation Centre, King's College London, 125 Coldharbour Ln, London, SE5 9NU, UK, Phone: +44 (0) 20 7848 5446, Fax: +44 (0) 20 7848 5298, manuel.mayr@kcl.ac.uk.

Disclosures. None.

Europe PMC Funders Author Manuscripts

Results—ECM-related glycoproteins were identified in left and right atrial appendages from the same patients. Several known glycosylation sites were confirmed. In addition, putative and novel glycosylation sites were detected. Upon enrichment for glycoproteins, peptides of the small leucine-rich proteoglycan decorin were consistently identified in the flow through. Out of all ECM proteins identified, decorin was found to be most fragmented. Within its protein core, eighteen different cleavage sites were identified. In contrast, no cleavage was observed for biglycan, the most closely related proteoglycan. Decorin processing differed between human ventricles and atria and was altered in disease. The C-terminus of decorin, important for the interaction with connective tissue growth factor, was predominantly detected in ventricles compared to atria. In contrast, atrial appendages from patients in persistent atrial fibrillation had higher levels of full-length decorin but also harbored a cleavage site that was not found in atrial appendages from patients in sinus rhythm. This cleavage site preceded the N-terminal domain of decorin that controls muscle growth by altering the binding capacity for myostatin. Myostatin expression was decreased in atrial appendages of patients with persistent atrial fibrillation and hearts of decorin null mice. A synthetic peptide corresponding to this decorin region dose-dependently inhibited the response to myostatin in cardiomyocytes and in perfused mouse hearts.

Conclusions—This proteomics study is the first to analyse the human cardiac ECM. Novel processed forms of decorin protein core, uncovered in human atrial appendages can regulate the local bioavailability of anti-hypertrophic and pro-fibrotic growth factors.

Keywords

Extracellular matrix; proteomics; mass spectrometry; atrial fibrillation; cardiovascular disease

Introduction

The importance of the ECM is increasingly being recognized, gradually overturning the concept that the cardiac ECM is inert. ECM proteins account for physiological properties of the cardiac tissue but also contribute to fibrosis and hypertrophy in disease. Fibrosis involves structural proteins but also matricellular proteins, predominantly glycoproteins. Due to the continuous need for dynamic adaptation in the heart, matricellular proteins are of particular importance. Previous studies have demonstrated that ECM deposition facilitates the development of ectopic pacemakers and late potentials as a result of inhomogeneous stimulus conduction, and can also lead to fluctuations in membrane potential.1 Thus, atrial fibrotic remodeling has been implicated as a potential therapeutic target in atrial fibrillation (AF).2

Proteomics offers the ability to quantify multiple proteins simultaneously without the constraints of antibodies. Most proteomics studies, including the ones on AF, investigated the cellular proteome. 3,4 We have previously developed a sequential extraction procedure to reduce cellular proteins before studying ECM remodelling in a porcine model of ischemia/reperfusion injury.5 No proteomics study has been conducted on the human cardiac ECM.

Therefore, the aims of the present study were fourfold: i) to provide a comprehensive characterisation of ECM proteins in human atrial appendages; ii) to interrogate protein glycosylation of matricellular proteins; iii) to explore regional differences in the cardiac

ECM composition; and iv) to interrogate ECM remodelling in the context of AF. We discovered extensive cleavage in the protein core of the proteoglycan decorin, a key constituent of the cardiac microenvironment. Decorin is a member of the small leucine-rich proteoglycan family (SLRPs)6,7 and regulates collagen fibrillogenesis as well as a variety of other ECM molecules involved in cell signalling.8 Processed forms of decorin detected in the human cardiac ECM had myostatin and connective tissue growth factor (CTGF) binding properties that might contribute to the pathophysiology of AF by regulating the bioavailability of growth factors.

Methods

An expanded Methods section is available in the online data supplement at http://circ.ahajournals.org.

Human cardiac tissue

All procedures involving use of human tissues were approved by the local Regional Ethics Committee Board. Written informed consent was obtained from all patients (n=65). Atrial samples were collected from patients undergoing cardiac surgery at St. George's School of Medicine (London, United Kingdom, REC number (06/Q0803/69) corresponding to EudraCT number: 2006-005272-40). Atrial tissue was obtained from the atrial appendages during cardiopulmonary bypass and just after cardioplegic arrest of the heart.4

ECM extraction

ECM protein enrichment was performed using our previously published 3-step extraction method, involving sequential incubation with 0.5M NaCl for 1 hr, 0.1% SDS for 16 hrs and a final incubation for 48 hr with 4M guanidine hydrochloride (GuHCl).5 Matched samples from both atria (n=5) were further enriched in ECM glycoproteins using a lectin-binding based protocol (i.e. wheat germ agglutinin and concanavalin A). GuHCl extracts (input), glycoprotein-enriched extracts and the flow-through were enzymatically deglycosylated. Gel electrophoresis for deglycosylated proteins was performed using 4-12% Bis-Tris gradient gels. Gels were fixed and silver stained. The entire gel lanes were excised and digested using trypsin.5 For direct glycopeptide identification, proteins were digested in solution without deglycosylation.

Mass spectrometry analyses

Liquid chromatography (LC) tandem mass spectrometry (MS/MS) acquisition was performed as previously described.9 MS/MS peak lists were matched to a human database using Mascot (version 2.3.01, Matrix Science). Two missed trypsin cleavages were allowed. An additional, "no enzyme" search was performed to identify peptides derived from non-tryptic cleavages. For the identification of the glycosylation sites, a direct glycopeptide strategy was pursued using a combination of different fragmentation modes on an Orbitrap Elite MS as published elsewhere.10

P(CAGA)12-luciferase reporter assay

HEK293 cells (ATCC) were transfected with the pGL3(CAGA)12 reporter plasmid. Recombinant mouse myostatin was added at a final concentration of 2.5nM ± decorin N-terminal peptides at different concentrations.11 The HEK293 cells were cultured for 24 hrs and were then lysed and luciferase activity was assayed.

Proton nuclear magnetic resonance ($^{+}$H-NMR) spectroscopy

Metabolites from mouse cardiac tissue were extracted using a methanol-based procedure. NMR spectra were acquired on a 700 MHz Bruker spectrometer using 9.3 kHz spectral width and 32 K data points with acquisition time of 1.67 s, relaxation delay of 5 s and 128 scans. The resulting spectra were processed to 65536 data points and corrected for phasing and zero referencing using NMRLab software.

Functional experiments

To test the biological effects of decorin peptides, neonatal rat cardiomyocytes were used for *in vitro* experiments, and hearts from 10-12 week-old C57BL/6J male mice were perfused in a Langendorff system. Details are given online.

Statistical analysis

Clinical characteristics are summarized as mean ± standard deviation (SD) or as percentages, and tested for differences across groups using unpaired t-tests for unequal variances or Fisher's exact tests. For all significance testing, a two-tailed $p<0.05$ was deemed significant.

Results

Glycoproteomic characterization of the ECM in human atria

Atrial appendages were obtained from patients undergoing coronary artery bypass grafting. The clinical characteristics and average atrial sizes of the patient cohort (n=14) are summarized in Table I in the online-only Data Supplement. ECM protein extracts were prepared as previously described5 and analysed using a high mass accuracy tandem mass spectrometer (Figure 1A). All identified extracellular proteins are listed in Table II in the online-only Data Supplement.

We also obtained left and right atrial appendages (LAA and RAA) from the same patients undergoing cardiac surgery (n=5 each) and added enrichment steps for glycoproteins and glycopeptides (Figure 1A). Peptides belonging to glycoproteins doubled upon enrichment for glycoproteins (Figure I in the online-only Data Supplement). The identified ECM-related glycoproteins as well as their distribution and abundance in the input (GuHCl extracts), glycoprotein-enriched fraction and unbound flow-through are shown in Table III and Figure II in the online-only Data Supplement, respectively. In the glycoprotein-enriched fraction, levels of nidogen 2 and cadherin 2 were more abundant in LAA, whereas latent transforming growth factor-beta binding protein 4, fibulin 2, lumican and vitronectin were increased in RAA (Figure 1B). The latter findings were validated by immunoblotting of the original input material (Figure 1C and 1D).

Next, we combined a direct MS/MS method with glycoprotein or glycopeptide enrichment strategies for the identification of the glycosylation sites (Figure 1A). In total, 65 N- and O-linked glycosylation sites were identified in 35 extracellular proteins. Several known glycosylation sites were confirmed. In addition, putative and novel glycosylation sites were detected (Table IV in the online-only Data Supplement). Identified N-glycoforms were mostly complex, some sialylated or core fucosylated. Minor presences of high mannose and hybrid glycans were observed. O-linked glycans were predominantly core 1 or 2 types with or without sialic acid.

Decorin processing in cardiac atria

Upon enrichment for glycoproteins, decorin peptides were consistently identified in the flow through (Figure 2A). Decorin has three consensus sequences for N-glycosylation at asparagine (Asn) 211, Asn262 and Asn303. Unlike other SLRPs, all N-glycosylation sites within decorin are located at the C-terminal half of the protein (Figure 2B). Glycosylation of decorin was confirmed by sequential deglycosylation and direct confirmation of its glycosylation sites by MS/MS (Figure III in the online-only Data Supplement). A comparison of the sequence coverage revealed that only peptides from the non-glycosylated N-terminal half of decorin were identified in the flow-through. In contrast, peptides spanning the entire sequence were obtained in the input and the glycoprotein-enriched fraction (Figure 2C). Trypsin is commonly used for protein digestion prior to MS/MS. Identification of cleavage sites produced by enzymes other than trypsin (“non-tryptic cleavages”) can be indicative of proteolysis. Few ECM proteins displayed evidence for non-tryptic cleavages (Table V in the online-only Data Supplement). For decorin, however, 18 cleavage sites were detected (Figure 3A), and 11.9% of all spectra were non-tryptic (Figure IVA in the online-only Data Supplement). Despite >50% sequence homology to decorin, only 1.2% of spectra for biglycan were non-tryptic. A sequence alignment between decorin and biglycan revealed that most cleavage sites are within non-conserved regions (Figure IVB in the online-only Data Supplement), suggesting that sequence variation provides selectivity to the proteolytic processing of cardiac matricellular proteins.

Decorin processing is region specific

To investigate regional differences in decorin processing, decorin levels were compared between LAA and left ventricles (LV). Antibodies raised against three different decorin regions were used: the N-terminus (Ile36-Leu86), the internal part (Leu136-Ile215) and the C-terminus (Phe312-Lys359) of decorin (Figure 3B). All three antibodies recognised recombinant human decorin as well as decorin in human cardiac tissue (Figure 3C). In agreement with its predicted molecular weight (Mw), decorin protein core migrated as a ~45-48 kDa doublet after removal of the glycosaminoglycan chain, but the three antibodies provided three different results (Figure 3C): according to the antibody recognizing the C-terminus, decorin was reduced in LAA compared to LV. The antibodies to the internal and the N-terminal part of decorin, however, did not confirm this result, but revealed a Mw difference of ~3kDa between decorin in LAA (45kDa) and LV (48kDa). C-terminal truncation of decorin may explain this apparent discrepancy. The C-terminal region of decorin inhibits the activity of CTGF. At the protein level, CTGF was more abundant in LV than LAA (Figure 3C, bottom panel) despite reduced transcript levels (Figure VA in the

online-only Data Supplement). A search for putative protease targets on decorin using the PROSPER database returned cathepsins K and G as the most likely effectors (Figure VB in the online-only Data Supplement) for the prominent cleavage at the C-terminus observed at Phe330-Ser331 (Figure IVB in the online-only Data Supplement). Transcript levels for cathepsin K were higher in LAA compared to LV (Figure VC in the online-only Data Supplement). Taken together, these data suggest region-specific processing of decorin in the human cardiac ECM that may affect the local retention of growth factors.

Decorin cleavage in AF

AF, the most common arrhythmia encountered in clinical practice, results in significant morbidity and mortality. To provide insight into the consequences of persistent AF on decorin protein abundance, we compared LAA from patients in sinus rhythm (SR) with those with postoperative AF (SR-AF) and in persistent AF (Figure 4A, Figure VIA in the online-only Data Supplement). Table VI and Table VII in the online-only Data Supplement summarize their clinical characteristics. At the transcript level, there was no change of decorin or CTGF expression in AF patients and patients who developed post-operative AF compared to SR controls (Figure VIB in the online-only Data Supplement). At the protein level, however, the structural damage inflicted by prolonged AF was associated with higher levels of the full-length and the 45kDa forms of decorin (Figure 4B). The shift in the Mw by 3kDa was similar to the one previously observed in LVs. Notably, CTGF protein levels were concurrently enhanced (Figure VIC in the online-only Data Supplement). Gene expression data using primers for the different regions of decorin support the notion that the processing of decorin occurs at the protein rather than the transcriptional level (Figure VID in the online-only Data Supplement). In contrast, decorin protein levels were found to be reduced in the SR-AF cohort compared to patients who maintained SR postoperatively (SR-SR) (Figure VII in the online-only Data Supplement).

Next, we interrogated the MS/MS data for potential cleavage sites.12 Non-tryptic peptides of decorin predominantly originated from four sites according to their absolute abundances: Val65-Gln66, Leu79-Pro80, Ser121-Pro122 and Phe330-Ser331. The latter cleavage site provides an explanation for the loss of detection with the antibody recognizing C-terminal epitopes. MS/MS spectra are shown in Figure VIIIA in the online-only Data Supplement, alongside elution times for the corresponding tryptic and non-tryptic peptides to exclude in-source fragmentation. Notably, an additional cleavage site (Ser49-Leu50) was found in AF (Figure 4C). This cleavage site is next to a N-terminal domain that inhibits myostatin11, a negative regulator of muscle cell growth. According to the absolute and relative intensities (Figure VIIIB in the online-only Data Supplement), the non-tryptic decorin peptide generated by proteolytic cleavage at Ser49-Leu50 was higher in AF patients. Structurally, this part of decorin constitutes a natively disordered region13, which hindered further assessment of putative protease cleavage sites14 (Figure IX in the online-only Data Supplement).

Inhibition of myostatin activity

Myostatin gene expression was significantly reduced in AF patients (Figure 5A). Thus, we hypothesized that this processed form of decorin protein core generated during AF could

directly interfere with myostatin bioactivity. Myostatin inhibits phosphorylation of AMPK and activates SMAD2/3 (Figure 5B). Via the SMAD2/3 cascade, myostatin controls cell growth and differentiation. By inhibiting AMPK phosphorylation, myostatin alters cardiac metabolism. We synthesised peptides corresponding to the N-terminal peptides of mouse and human decorin (Figure XA in the online-only Data Supplement) and tested their activity in a reporter gene assay using HEK293-cells transfected with CAGA-luciferase plasmid. CAGA boxes are recognised by SMAD3 on the promoter regions of SMAD3-responsive genes, and therefore this technique screens SMAD3 activity. Incubation of transfected cells with 2.5nM myostatin triggered the activation of pathways downstream of the myostatin receptor as evidenced by increased luciferase activity. Addition of the synthetic N-terminal peptide (murine decorin AA 42-71, cleaved N-terminus) dose-dependently reduced this response (rho=-1.00, $p<0.01$) (Figure 5C). A longer decorin peptide (mouse AA 31-71, full N-terminus) was not as effective (rho=-0.83, $p=0.04$) (Figure XB in the online-only Data Supplement). Next, cell size was measured on isolated neonatal rat cardiomyocytes (Figure 5D). The shorter N-terminal peptide mediated a strong repression of myostatin activity as evidenced by an increase in cell size upon hypertrophy stimuli (i.e. isoproterenol and phenylephrine) (Figure 5E and 5F; Figure XC in the online-only Data Supplement). Thus, decorin cleavage generates peptides with anti-myostatin activity.

Decorin null mice

The interaction of decorin with myostatin was further confirmed in hearts obtained from decorin null ($DCN^{-/-}$) mice. Decorin deficiency resulted in a ≈50% reduction of myostatin expression (Figure 6A). Related ECM proteins showed no changes in abundance, but decorin deficiency was accompanied by a marked increase in SMAD2 phosphorylation (Figure 6B). Metabolic consequences of decorin deficiency were evident in metabolic profiles obtained by $^{+}$H-NMR spectroscopy (Figure 6C; Figure XIA in the online-only Data Supplement). Levels of glutamine, succinate, aspartate and nicotinamide adenine dinucleotides (NAD^{+}, NADH) were elevated in decorin null hearts, as compared to littermate controls (Figure 6D). In isolated cardiomyocytes, myostatin reduced AMPK phosphorylation, a master regulator for cardiac energy metabolism (Figure 6E). This myostatin effect was reversed by preincubation with decorin peptides corresponding to the myostatin-binding region in mouse and human (Figure 6F; Figure XIB and XIC in the online-only Data Supplement). A similar inhibitory effect of the N-terminal decorin peptide on myostatin signalling was observed in Langendorff hearts (Figure 6G and 6H; Figure XID in the online-only Data Supplement).

Discussion

By applying a novel proteomics approach to human atria, fundamental insights were obtained about the composition and the proteolytic processing of the human cardiac ECM, which has not been analyzed by proteomics thus far. Using proteomics in combination with metabolomics, we have previously shown that discordant metabolic alterations are evident in individuals susceptible to postoperative AF.4 We now identify endogenous decorin cleavage products in AF that may contribute to atrial remodelling and play a previously unrecognized

role in the susceptibility or perpetuation of arrhythmias by altering the local bioavailability of growth factors, such as CTGF and myostatin.

Glycoproteomics of the cardiac ECM

Thus far, proteomic studies of cardiac disease focussed mainly on evaluating differences in protein abundance4,5, in phosphorylation9,15 and in redox-modifications.16 However, alterations in glycosylation patterns and protein degradation are known to occur in disease.17 Our study characterizes, for the first time, ECM proteins in human atria using state-of-the-art glycoproteomics. Previously, Parker *et al*18 used glycoproteomics in rat hearts and characterised glycan composition after removal of the sugar moieties from the peptides. In this study, we analysed intact glycopeptides. Unlike conventional studies, in which ECM proteins are analysed by antibodies, proteomics does not require *a priori* decisions on which ECM proteins to study, and MS/MS is not dependent on the recognition of epitopes. Epitopes become masked i.e. by glycosylation or destroyed by proteolytic cleavage. These inherent constraints of antibody-based detection can lead to misinterpretations as demonstrated by the three immunoblots for decorin presented in Figure 3C.

Decorin and other SLRPs

Decorin is a member of SLRPs, a family of 18 structurally related ECM proteins. After synthesis, SLRPs are secreted into the extracellular space and exert diverse roles as biologically active regulators of the ECM.19 Similar to biglycan, decorin has a horseshoe shape and binds to collagen fibres to control their shape, size and distribution. Decorin and biglycan share >50% sequence identity, and have chemically similar amino acid substitutions at most other positions.20 Yet, decorin, but not biglycan, was subject to extensive proteolytic processing in human atria. Despite the structural and functional similarities of SLRPs, decorin is located in the interstitial ECM whereas biglycan is mainly associated to collagens in the pericellular regions.21 A sequence alignment between decorin and biglycan revealed that most cleavage sites in decorin mapped to non-conserved regions. Thus, specific cleavage sites might endow decorin with additional functional properties in the heart.

Biological activity of ECM cleavage products

Besides its role in ECM assembly, decorin has structural moieties that recognize not only collagens but also growth factors and cell surface receptors, affecting their activity and bioavailability.19,22 The regulatory mechanisms involve interactions with sugar residues or specific domains within the core protein.23 It is noteworthy that amongst all SLRPs, decorin had the highest number of non-tryptic cleavage sites, which were predominantly located on the N-terminal half of the protein. In general, the N-terminus and the C-terminus of SLRPs offer the highest variability for interaction partners.22 The decorin peptides within the N-terminal half have anti-myostatin properties.11 An abundant cleavage site at the C-terminus (Phe330-Ser331) gives rise to a peptide with CTGF-binding properties.24 The known cleavage sites of decorin as well as the non-tryptic cleavages identified in atrial appendages and their relation to binding sequences for collagen and growth factors are summarized in Figure XII in the online-only Data Supplement.

C-terminal decorin peptides bind CTGF

The C-terminal tail of decorin, also known as the cysteine-rich “ear”, is involved in ligand-binding regulation and conformational stability via two cysteines at positions 313 and 346. A point mutation within this region is the genetic cause for congenital hereditary stromal dystrophy of the cornea and linked to abnormal fibrillogenesis.25 The abundant cleavage site at position Phe330-Ser331 results in a truncated form of decorin (loss of 3 kDa). C-terminal truncation of decorin was predominantly observed in LAA and to a lesser extent in LV. Importantly, a synthetic decorin peptide within LRR12 (i.e. Gln335-Lys359) has been shown to bind CTGF and attenuate fibrosis.24 Thus, C-terminal truncation may result in diminished collagen-binding ability and repression of CTGF activity in human atria with their lower mechanical load and decreased stiffness compared to LV (Figure 7).

N-terminal decorin peptides regulate myostatin

At the N-terminus, four cysteine residues form a disulfide knot (Cys54-Cys60 and Cys58-Cys67) that buries the hydrophobic core of the first leucine-rich repeat (LRR1). Binding of Zn^{2+} to this region results in a conformational change required for myostatin binding.26 Equivalent biglycan moieties do not bind myostatin.26,27 Myostatin, a potent antagonist to hypertrophic stimuli28, is synthesized as inactive protein with a N-terminal propeptide. After activation, myostatin is regulated via non-covalent binding to its propeptide, forming a latent complex.29 Our experiments demonstrated a markedly lower expression of myostatin in hearts of decorin null mice, supporting the notion of a myostatin-decorin feedback loop. In cardiomyocytes, myostatin regulates at least two pathways downstream of the activin receptor (Figure 5B): (i) Co-incubation of myostatin with the N-terminal decorin peptide lead to inhibition of SMAD2/3 activity in a dose-dependent manner. SMAD3 activation via myostatin represses muscle cell growth.30 When cardiomyocytes were treated with increasing concentrations of the N-terminal decorin peptide, the effect of myostatin on cell size was reversed. In line with these *in vitro* findings, SMAD2 phosphorylation was increased in hearts of decorin null mice. (ii) By inhibiting AMPK phosphorylation via activin receptor and TAK1, myostatin regulates cardiac energy homeostasis.31 AMPK is a crucial energy sensor with a phosphorylation site in its activation loop at threonine 172 (Thr_{172}).32 In *in vitro* and *ex vivo* experiments, both the murine and the human N-terminal peptides of decorin maintained phosphorylation of AMPK at Thr_{172} in the presence of myostatin. In hearts of decorin null mice, with reduced myostatin levels, NMR spectroscopy profiling revealed changes in metabolites linked to mitochondrial metabolism and an accumulation of nicotinamide adenine dinucleotides. Activation of AMPK increases ATP production mostly by enhancing oxidative metabolism leading to a gradual increase in NAD^+ levels as a consequence of fatty acid oxidation.33

Decorin in patients with AF

In human AF, we observed an additional decorin cleavage site next to the myostatin-binding region (Figure 7, position Ser49-Leu50).11 This cleavage site generates a decorin form devoid of the glycosaminoglycan chain at Ser34.14 We demonstrated that the resulting peptide suppresses myostatin activity and increases cardiomyocyte size. Notably, in a goat model of pacing-induced AF, changes in cellular substructures were accompanied by an

increase in myocyte size (up to 195%).34 The additional cleavage site in AF releases decorin peptides that only contain the myostatin-binding region and are therefore less likely to interact with other binding partners. In comparison to other regulators of myostatin activity, i.e. myostatin propeptide and follistatin35, decorin is abundant and readily available within the cardiac ECM. Thus, its cleavage products may constitute an important local regulatory mechanism of myostatin activity.

Evidence in preclinical models

Inhibition of myostatin by cardiac-specific overexpression of the myostatin propeptide induced enlarged atria and AF in the transgenic mice.36 Similarly, mice overexpressing microRNA-208a, a “myomiR” enriched in hearts, developed spontaneous AF. Besides thyroid hormone receptor-associated protein 1, myostatin was identified as a regulatory target of microRNA-208a.37 Similarly, AMPK signalling, one of the key downstream signalling pathways of myostatin, has been implicated as a mechanism for AF in mice with cardiac-specific deletion of liver kinase B1.38 Taking together, these data provide *in vivo* evidence that loss of myostatin activity and dysregulation of AMPK signaling can act as a substrate for AF, at least in mice.

Study limitations

Our proteomics findings in clinical samples do not directly prove a decorin-mediated effect on atrial myostatin signaling. While local injection of decorin peptides in skeletal muscle increased muscle mass11, *in vivo* studies are required to further explore the role of decorin cleavage products in cardiac disease, i.e. the specificity of the interaction and the location of the effects. Decorin has many binding partners.8 Thus, the genetic deletion of decorin in mice may have pleiotropic effects. Lectin enrichment of glycoproteins presents selectivity bias towards specific glycoforms, and high Mw glycoproteins in basement membranes, i.e. collagens, laminins, and perlecan, are barely re-solubilised by buffers compatible with the affinity enrichment of glycoproteins. The direct glycopeptide method employed in this study identifies the peptide sequence, the glycosite, and the glycan mass but the glycan composition is only calculated based on accurate mass and the glycan structure remains unresolved. Emerging technologies combining MS with glycan structural data are yet to be applied to the human and cardiac contexts.39 Moreover, non-tryptic cleavage sites at positions containing lysine or arginine will be missed by digestion with trypsin. Advances in positional proteomics will help to better characterize proteolytic cleavage in cardiac disease. 40

Conclusions

The glycoproteomic analysis of atrial appendages allowed, for the first time, a detailed analysis of human cardiac ECM proteins. It examined differences in the ECM composition between RAA and LAA; confirmed putative and revealed new glycosylation sites in the cardiac ECM; and identified decorin-derived cleavage products that can act as local regulators of growth factor activity. Proteomic workflows, as outlined in this study, will be essential to explore the different aspects of ECM remodelling in cardiovascular disease, as exemplified by the observed changes in decorin processing during structural remodelling in persistent AF.

Europe PMC Funders Author Manuscripts

Supplementary Material

Refer to Web version on PubMed Central for supplementary material.

Acknowledgments

Sources of funding. Prof. Mayr is a Senior Research Fellow of the British Heart Foundation (FS/13/2/29892). Dr. Zampetaki is an Intermediate Research Fellow of the British Heart Foundation. Dr. Willeit is an Erwin Schrödinger Fellow in Epidemiology sponsored by the Austrian Science Fund (J 3679-B13). Prof. Fischer obtained funding from the Deutsche Forschungsgemeinschaft (DFG/SFB 1116). This work was supported by King's British Heart Foundation Centre and the National Institute for Health Research (NIHR) Biomedical Research Centre based at Guy's and St Thomas' NHS Foundation Trust and King's College London in partnership with King's College Hospital. There is no relationship with industry.

Abbreviations and Acronyms

AF	atrial fibrillation
ECM	extracellular matrix
LAA	left atrial appendages
LC	liquid chromatography
MS/MS	tandem mass spectrometry
Mw	molecular weight
RAA	right atrial appendages
SR	sinus rhythm
SR-AF	postoperative AF

References

1. Pellman J, Lyon RC, Sheikh F. Extracellular matrix remodeling in atrial fibrosis: mechanisms and implications in atrial fibrillation. J Mol Cell Cardiol. 2010; 48:461–467. [PubMed: 19751740]
2. Dawson K, Wakili R, Ordög B, Clauss S, Chen Y, Iwasaki Y, Voigt N, Qi XY, Sinner MF, Dobrev D, Kääb S, et al. MicroRNA29: a mechanistic contributor and potential biomarker in atrial fibrillation. Circulation. 2013; 127:1466–1475. [PubMed: 23459615]
3. Chiang DY, Lebesgue N, Beavers DL, Alsina KM, Damen JM, Voigt N, Dobrev D, Wehrens XH, Scholten A. Alterations in the interactome of serine/threonine protein phosphatase type-1 in atrial fibrillation patients. J Am Coll Cardiol. 2015; 65:163–173. [PubMed: 25593058]
4. Mayr M, Yusuf S, Weir G, Chung YL, Mayr U, Yin X, Ladroue C, Madhu B, Roberts N, De Souza A, Fredericks S, et al. Combined metabolomic and proteomic analysis of human atrial fibrillation. J Am Coll Cardiol. 2008; 51:585–594. [PubMed: 18237690]
5. Barallobre-Barreiro J, Didangelos A, Schoendube FA, Drozdov I, Yin X, Fernández-Caggiano M, Willeit P, Puntmann VO, Aldama-López G, Shah AM, Doménech N, et al. Proteomics analysis of cardiac extracellular matrix remodeling in a porcine model of ischemia/reperfusion injury. Circulation. 2012; 125:789–802. [PubMed: 22261194]
6. Jahanyar J, Joyce DL, Southard RE, Loebe M, Noon GP, Koerner MM, Torre-Amione G, Youker KA. Decorin-mediated transforming growth factor-beta inhibition ameliorates adverse cardiac remodeling. J Heart Lung Transplant. 2007; 26:34–40. [PubMed: 17234515]

7. Melchior-Becker A, Dai G, Ding Z, Schäfer L, Schrader J, Young MF, Fischer JW. Deficiency of biglycan causes cardiac fibroblasts to differentiate into a myofibroblast phenotype. J Biol Chem. 2011; 286:17365–17375. [PubMed: 21454527]
8. Neill T, Schaefer L, Iozzo RV. Decorin: a guardian from the matrix. Am J Pathol. 2012; 181:380–387. [PubMed: 22735579]
9. Yin X, Cuello F, Mayr U, Hao Z, Hornshaw M, Ehler E, Avkiran M, Mayr M. Proteomics analysis of the cardiac myofilament subproteome reveals dynamic alterations in phosphatase subunit distribution. Mol Cell Proteomics. 2010; 9:497–509. [PubMed: 20037178]
10. Yin X, Bern M, Xing Q, Ho J, Viner R, Mayr M. Glycoproteomic analysis of the secretome of human endothelial cells. Mol Cell Proteomics. 2013; 12:956–978. [PubMed: 23345538]
11. Guiraud S, van Wittenberghe L, Georger C, Scherman D, Kichler A. Identification of decorin derived peptides with a zinc dependent anti-myostatin activity. Neuromuscul Disord. 2012; 22:1057–1068. [PubMed: 22854012]
12. Stegemann C, Didangelos A, Barallobre-Barreiro J, Langley SR, Mandal K, Jahangiri M, Mayr M. Proteomic identification of matrix metalloproteinase substrates in the human vasculature. Circ Cardiovasc Genet. 2013; 6:106–117. [PubMed: 23255316]
13. Scott PG, McEwan PA, Dodd CM, Bergmann EM, Bishop PN, Bella J. Crystal structure of the dimeric protein core of decorin, the archetypal small leucine-rich repeat proteoglycan. Proc Natl Acad Sci U S A. 2004; 101:15633–15638. [PubMed: 15501918]
14. Daquinag AC, Zhang Y, Amaya-Manzanares F, Simmons PJ, Kolonin MG. An isoform of decorin is a resistin receptor on the surface of adipose progenitor cells. Cell Stem Cell. 2011; 9:74–86. [PubMed: 21683670]
15. Husberg C, Agnetti G, Holewinski RJ, Christensen G, Van Eyk JE. Dephosphorylation of cardiac proteins in vitro - a matter of phosphatase specificity. Proteomics. 2012; 12:973–978. [PubMed: 22522803]
16. Charles RL, Burgoyne JR, Mayr M, Weldon SM, Hubner N, Dong H, Morisseau C, Hammock BD, Landar A, Eaton P. Redox regulation of soluble epoxide hydrolase by 15-deoxy-delta-prostaglandin J2 controls coronary hypoxic vasodilation. Circ Res. 2011; 108:324–334. [PubMed: 21164107]
17. Ungar D. Golgi linked protein glycosylation and associated diseases. Semin Cell Dev Biol. 2009; 20:762–769. [PubMed: 19508859]
18. Parker BL, Palmisano G, Edwards AV, White MY, Engholm-Keller K, Lee A, Scott NE, Kolarich D, Hambly BD, Packer NH, Larsen MR, et al. Quantitative N-linked glycoproteomics of myocardial ischemia and reperfusion injury reveals early remodeling in the extracellular environment. Mol Cell Proteomics. 2011; 10:M110.006833.
19. Chen S, Birk DE. The regulatory roles of small leucine-rich proteoglycans in extracellular matrix assembly. FEBS J. 2013; 280:2120–2137. [PubMed: 23331954]
20. Fisher LW, Termine JD, Young MF. Deduced protein sequence of bone small proteoglycan I (biglycan) shows homology with proteoglycan II (decorin) and several nonconnective tissue proteins in a variety of species. J Biol Chem. 1989; 264:4571–4576. [PubMed: 2647739]
21. Bianco P, Fisher LW, Young MF, Termine JD, Robey PG. Expression and localization of the two small proteoglycans biglycan and decorin in developing human skeletal and non-skeletal tissues. J Histochem Cytochem. 1990; 38:1549–1563. [PubMed: 2212616]
22. Iozzo RV, Schaefer L. Proteoglycans in health and disease: novel regulatory signaling mechanisms evoked by the small leucine-rich proteoglycans. FEBS J. 2010; 277:3864–3875. [PubMed: 20840584]
23. Tocchi A, Parks WC. Functional interactions between matrix metalloproteinases and glycosaminoglycans. FEBS J. 2013; 280:2332–2341. [PubMed: 23421805]
24. Vial C, Gutiérrez J, Santander C, Cabrera D, Brandan E. Decorin interacts with connective tissue growth factor (CTGF)/CCN2 by LRR12 inhibiting its biological activity. J Biol Chem. 2011; 286:24242–24252. [PubMed: 21454550]
25. Bredrup C, Knappskog PM, Majewski J, Rødahl E, Boman H. Congenital stromal dystrophy of the cornea caused by a mutation in the decorin gene. Invest Ophthalmol Vis Sci. 2005; 46:420–426. [PubMed: 15671264]

26. Yang VW, LaBrenz SR, Rosenberg LC, McQuillan D, Höök M. Decorin is a Zn2+ metalloprotein. J Biol Chem. 1999; 274:12454–12460. [PubMed: 10212220]
27. Miura T, Kishioka Y, Wakamatsu J, Hattori A, Hennebry A, Berry CJ, Sharma M, Kambadur R, Nishimura T. Decorin binds myostatin and modulates its activity to muscle cells. Biochem Biophys Res Commun. 2006; 340:675–680. [PubMed: 16380093]
28. Morissette MR, Cook SA, Foo S, McKoy G, Ashida N, Novikov M, Scherrer-Crosbie M, Li L, Matsui T, Brooks G, Rosenzweig A. Myostatin regulates cardiomyocyte growth through modulation of Akt signaling. Circ Res. 2006; 99:15–24. [PubMed: 16763166]
29. Jiang MS, Liang LF, Wang S, Ratovitski T, Holmstrom J, Barker C, Stotish R. Characterization and identification of the inhibitory domain of GDF-8 propeptide. Biochem Biophys Res Commun. 2004; 315:525–531. [PubMed: 14975732]
30. Breitbart A, Auger-Messier M, Molkentin JD, Heineke J. Myostatin from the heart: local and systemic actions in cardiac failure and muscle wasting. Am J Physiol Heart Circ Physiol. 2011; 300:H1973–1982. [PubMed: 21421824]
31. Biesemann N, Mendler L, Wietelmann A, Hermann S, Schäfers M, Krüger M, Boettger T, Borchardt T, Braun T. Myostatin regulates energy homeostasis in the heart and prevents heart failure. Circ Res. 2014; 115:296–310. [PubMed: 24807786]
32. Hardie DG, Ross FA, Hawley SA. AMPK: a nutrient and energy sensor that maintains energy homeostasis. Nat Rev Mol Cell Biol. 2012; 13:251–262. [PubMed: 22436748]
33. Cantó C, Gerhart-Hines Z, Feige JN, Lagouge M, Noriega L, Milne JC, Elliott PJ, Puigserver P, Auwerx J. AMPK regulates energy expenditure by modulating NAD+ metabolism and SIRT1 activity. Nature. 2009; 458:1056–1060. [PubMed: 19262508]
34. Ausma J, Wijffels M, Thoné F, Wouters L, Allessie M, Borgers M. Structural changes of atrial myocardium due to sustained atrial fibrillation in the goat. Circulation. 1997; 96:3157–3163. [PubMed: 9386188]
35. Lee SJ, McPherron AC. Regulation of myostatin activity and muscle growth. Proc Natl Acad Sci U S A. 2001; 98:9306–9311. [PubMed: 11459935]
36. Rosenberg MA, Das S, Pinzon PQ, Knight AC, Sosnovik DE, Ellinor PT, Rosenzweig A. A novel transgenic mouse model of cardiac hypertrophy and atrial fibrillation. J Atr Fibrillation. 2012; 2:1–15. [PubMed: 23243484]
37. Callis TE, Pandya K, Seok HY, Tang RH, Tatsuguchi M, Huang ZP, Chen JF, Deng Z, Gunn B, Shumate J, Willis MS, et al. MicroRNA-208a is a regulator of cardiac hypertrophy and conduction in mice. J Clin Invest. 2009; 119:2772–2786. [PubMed: 19726871]
38. Ikeda Y, Sato K, Pimentel DR, Sam F, Shaw RJ, Dyck JRB, Walsh K. Cardiac-specific deletion of LKB1 leads to hypertrophy and dysfunction. J Biol Chem. 2009; 284:35839–35849. [PubMed: 19828446]
39. Parker BL, Thaysen-Andersen M, Solis N, Scott NE, Larsen MR, Graham ME, Packer NH, Cordwell SJ. Site-specific glycan-peptide analysis for determination of N-glycoproteome heterogeneity. J Proteome Res. 2013; 12:5791–800. [PubMed: 24090084]
40. Eckhard U, Marino G, Butler GS, Overall CM. Positional proteomics in the era of the human proteome project on the doorstep of precision medicine. Biochimie. 2016; 122:110–8. [PubMed: 26542287]

Europe PMC Funders Author Manuscripts

Clinical Perspective

What is new?

- We used proteomics to analyse the extracellular matrix in human atrial appendages. By using novel mass spectrometry methods, we provide the first comprehensive characterisation of human cardiac extracellular matrix proteins, including the identification of glycosylation sites.
- We found that decorin, a small and leucine-rich proteoglycan, is truncated in atria compared to ventricles resulting in the loss of the binding site for connective tissue growth factor. In atrial fibrillation, decorin is increased but an additional cleavage site gives rise to peptides with myostatin-binding properties. These decorin peptides antagonize myostatin.

What are the clinical implications?

- Atrial fibrillation is the most common arrhythmia encountered in clinical practice and myostatin inhibition has been implicated as a substrate for atrial fibrillation. Myostatin expression was reduced in patients with atrial fibrillation and in hearts from decorin null mice.
- Peptides generated from the cleavage of extracellular matrix proteins such as decorin constitute a local regulatory mechanism for the bioactivity and bioavailability of growth factors in human cardiac tissue.

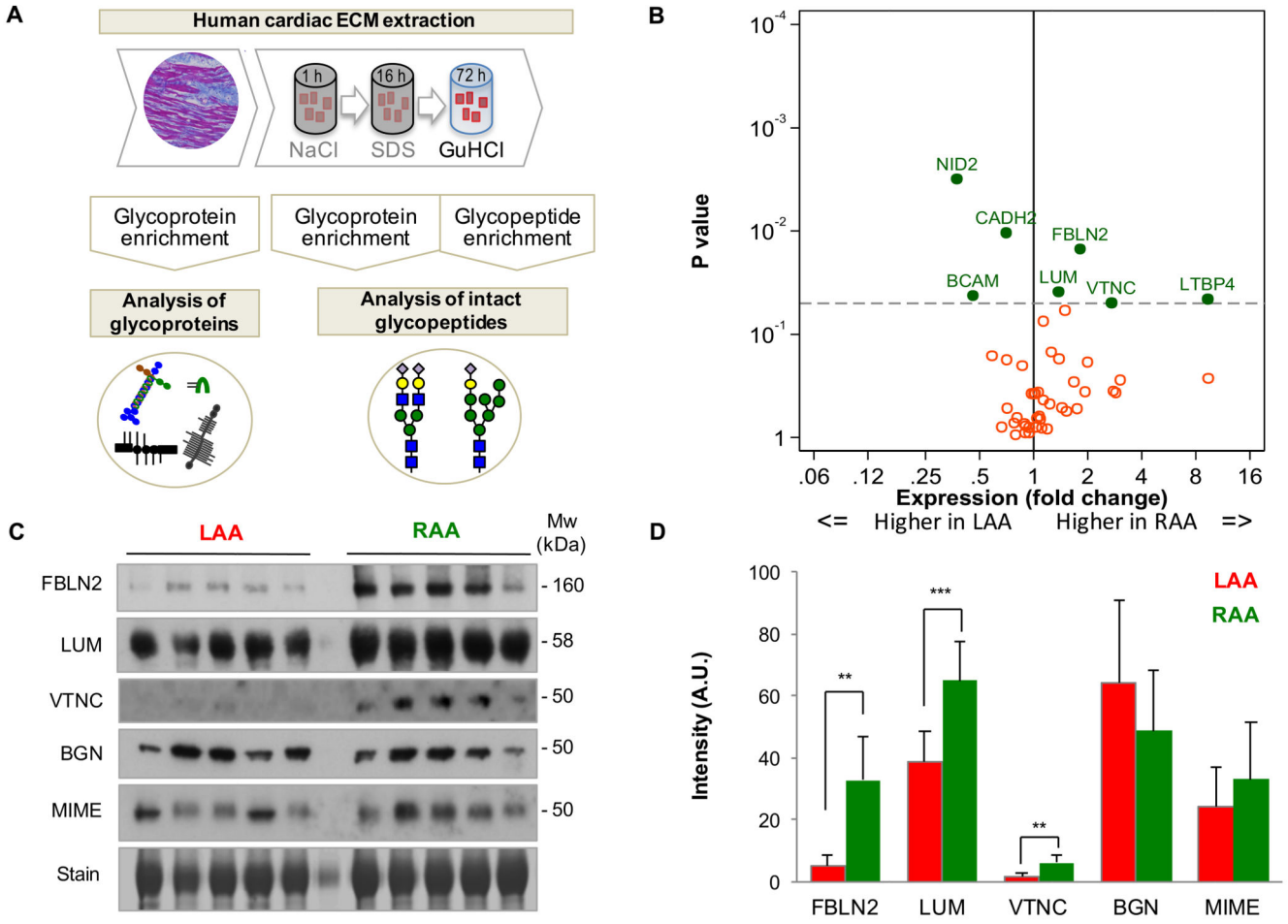

Figure 1. Glycoproteomics of the human cardiac ECM.

A) Atrial appendages were collected from patients in SR during cardiac surgery and subject to a decellularization-based three-step extraction for ECM proteins. First, GuHCl extracts were analyzed by LC-MS/MS. Then, ECM extracts were enriched for glycoproteins. The glycoprotein-enriched and unbound flow-through fractions were analysed by LC-MS/MS. Finally, enrichment was performed for glycoproteins as well as glycopeptides for direct glycopeptide identification by LC-MS/MS. **B)** Comparison of ECM-related glycoproteins in LAA and RAA (n=5, each). LTBP4 denotes latent transforming growth factor-beta binding protein 4; VTNC, vitronectin; FBLN2, fibulin 2; LUM, lumican; NID2, nidogen 2; CADH2, cadherin 2; BCAM, basal cell adhesion molecule. **C)** Validation by immunoblotting. Biglycan, mimecan (MIME) and Coomassie staining were included as controls. **D)** Quantification by densitometry. Bars represent mean ± SD. **p<0.01; ***p<0.001; A.U., arbitrary units.

Europe PMC Funders Author Manuscripts

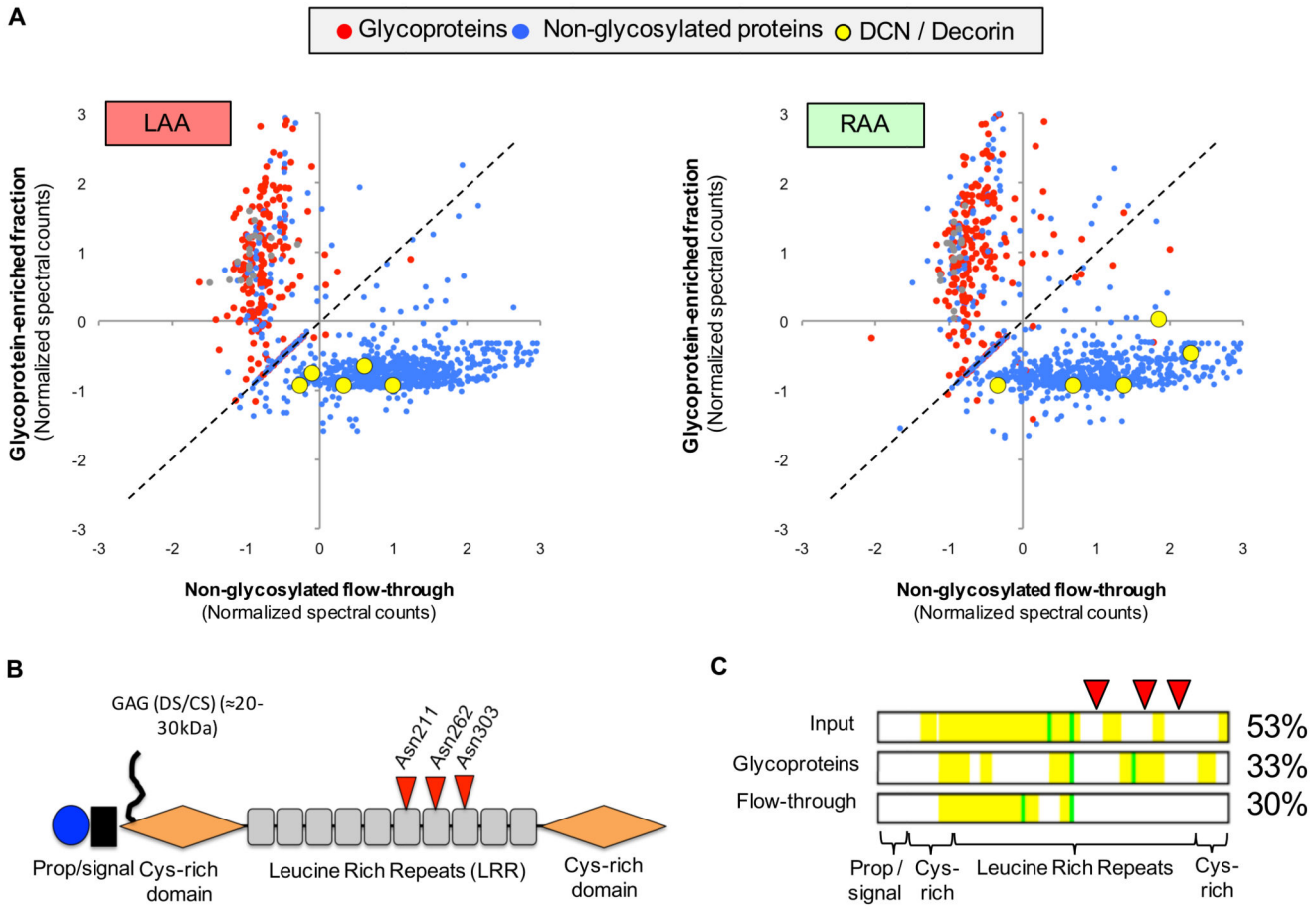

Figure 2. Decorin after glycoprotein enrichment.

A) Proteomic comparison of the glycoprotein-enriched fraction and the flow-through. Relative abundances of glycoproteins (red dots) and non-glycosylated proteins (blue dots) are plotted for LAA and RAA (n=5, each). Decorin was the only glycoprotein consistently detected among the non-glycosylated proteins in the flow-through (yellow dots). **B)** The C-terminal half of decorin has three N-glycosylation sites (red triangles). **C)** According to the sequence coverage (yellow colour) in the three different fractions (input, glycoprotein-enriched fraction, non-glycosylated flow-through), only N-terminal (non-glycosylated) decorin peptides were identified in the flow-through.

Europe PMC Funders Author Manuscripts

Europe PMC Funders Author Manuscripts

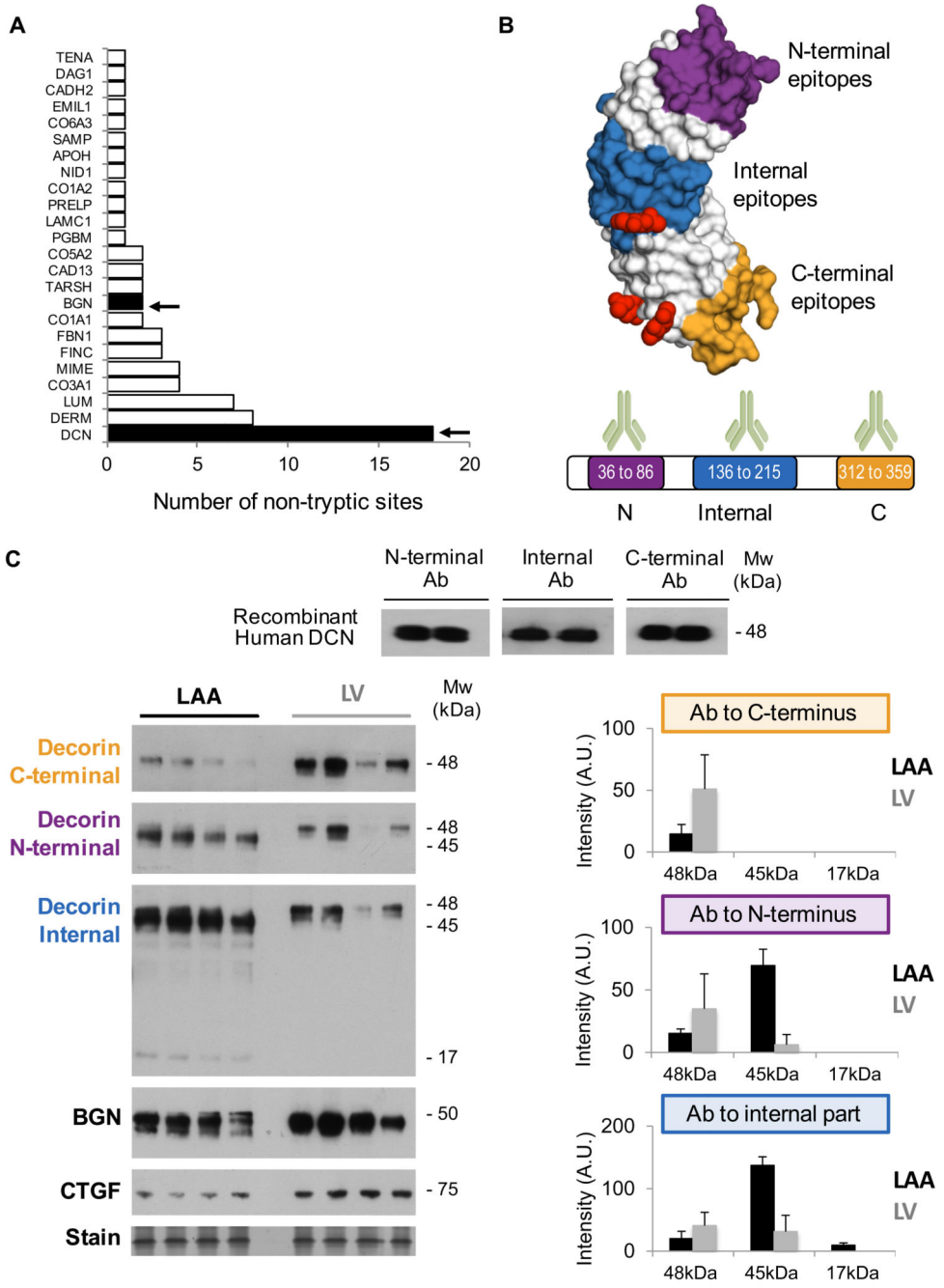

Figure 3. Decorin processing in atrial tissue.

A) Decorin (DCN) showed the highest number of non-tryptic cleavage sites among all ECM proteins identified. Biglycan (BGN) is highlighted for comparison. **B)** Three different antibodies recognizing different epitopes were used to detect decorin. Numbers indicate amino acid positions. **C)** Comparison of LAA and LV. Note the C-terminal truncation of decorin in LAA compared to LV from non-failing hearts (Mw shift from 48kDa to 45kDa). The apparent reduction of decorin levels in LAA with the C-terminal antibody was not corroborated by antibodies to N-terminal and internal epitopes. Instead, they revealed a loss

of ~3kDa in LAA compared to LV. Biglycan, a highly homologous SLRP, showed no such shift in Mw. The graphs show the densitometry results from immunoblots based on antibodies against three different decorin epitopes. Bars represent mean ± SD. A.U., arbitrary units.

Europe PMC Funders Author Manuscripts

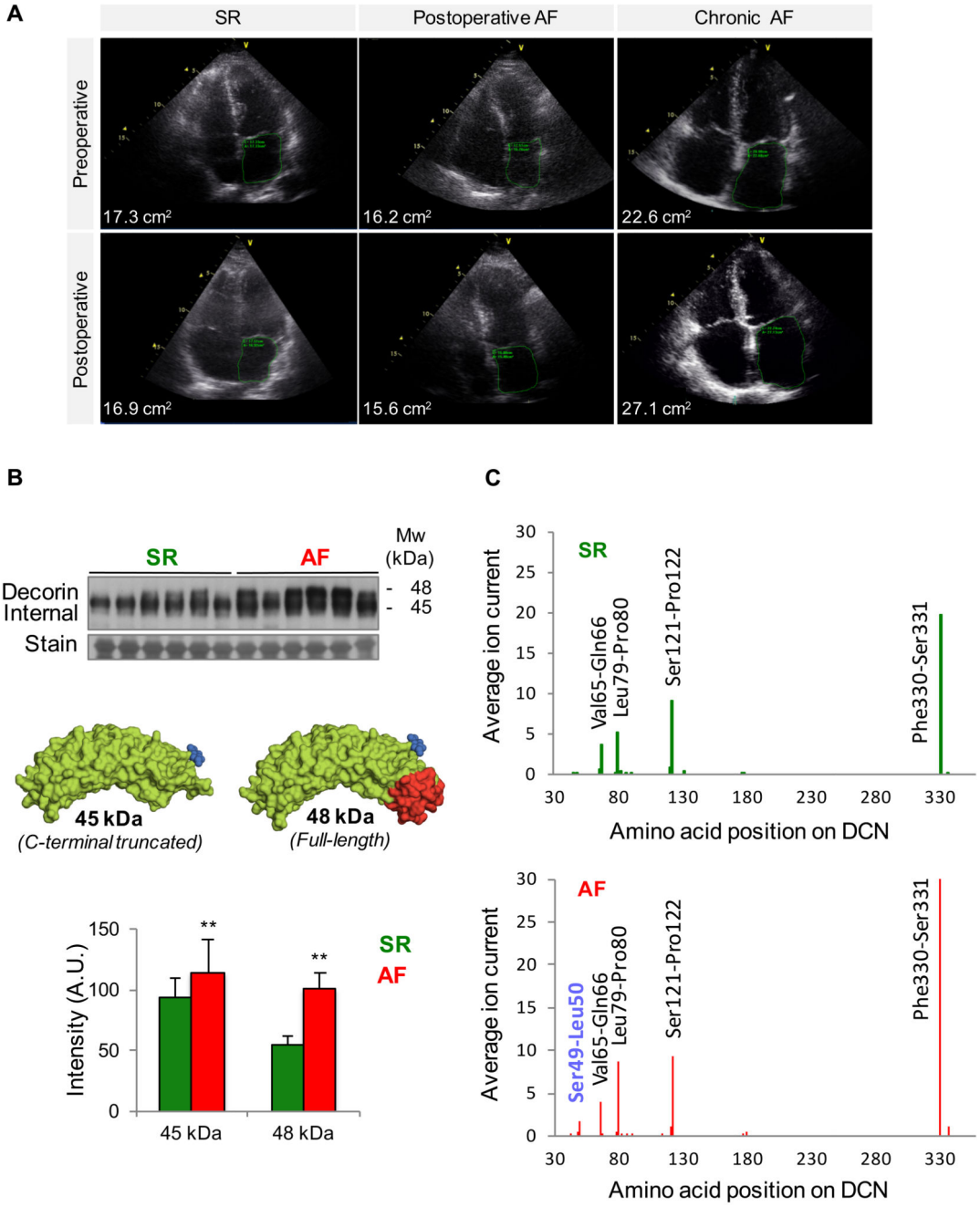

Figure 4. Decorin processing in AF.

A) Representative pre-operative and postoperative echocardiography images from patients who stayed in SR throughout surgery and patients who developed postoperative AF. Rightmost panels depict left atrial structural remodeling observed in a patient with permanent, chronic AF after a 5-year follow-up. **B)** Immunoblotting for decorin in GuHCl extracts from LAA samples. Decorin was more abundant in AF than SR patients, and both bands (C-terminally truncated decorin at 45kDa and full-length at 48kDa) became detectable. The bottom chart shows the quantification (mean ± SD) in SR and AF patients

(n=6, each) with the antibody against the internal region. **p<0.01 **C)** GuHCl extracts (n=6, each group) were analysed using LC-MS/MS. After a search using no enzyme, non-tryptic decorin peptides were identified and quantified. In addition to the four main cleavage sites of decorin in SR, a N-terminal cleavage site at position Ser49-Leu50 was detected in AF.

Europe PMC Funders Author Manuscripts

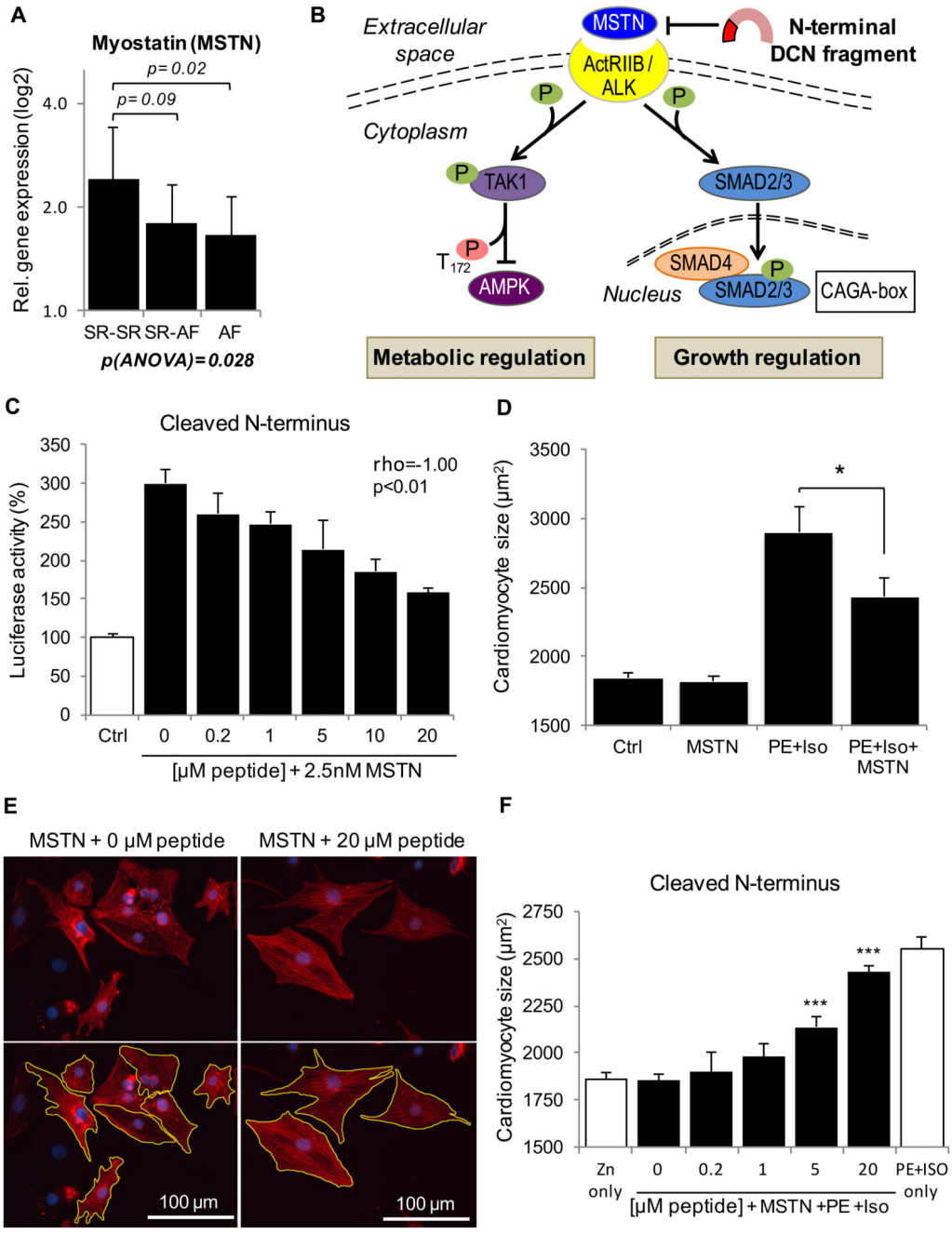

Figure 5. Decorin peptides bind myostatin.

A) qPCR analysis for myostatin expression in additional samples (SR-SR=14, SR-AF=10, AF=13). Bars represent mean ± SD. **B)** Schematic illustration of two downstream signaling pathways of myostatin (MSTN). “ActRIIB/ALK” denotes Activin receptor type-2B (ActRIIB)/ activin receptor-like kinase (ALK) receptor complex; “TAK1” transforming growth factor beta-activated kinase 1. **C)** Repression of MSTN-SMAD3 signaling. A synthetic N-terminal peptide of mouse decorin (amino acids 42-71 corresponding to the peptide generated by the Ser49-Leu50 cleavage site in humans) inhibited the CAGA-

Europe PMC Funders Author Manuscripts

luciferase reporter activity in a dose-dependent manner. The trend for the effect was calculated based on Spearman's correlation (rho, ρ). Bars are mean ± SD of triplicate experiments. **D)** Effect on rat cardiomyocytes. MSTN represses hypertrophy induced by pre-treatment with isoproterenol (Iso) and phenylephrine (PE). Cardiomyocyte size is given as mean ± standard error of the mean (SEM). **E)** Cardiomyocyte size was calculated after defining the cell perimeter to integrate the area (see bottom panels). **F)** The decorin N-terminal peptide attenuated the MSTN effect dose-dependently (0-20μM). Cardiomyocyte size is given as mean ± SEM based on a total of 300-400 cell measurements per experimental condition and compared to a control without decorin N-terminal peptide. *p<0.05; ***p<0.001.

Europe PMC Funders Author Manuscripts

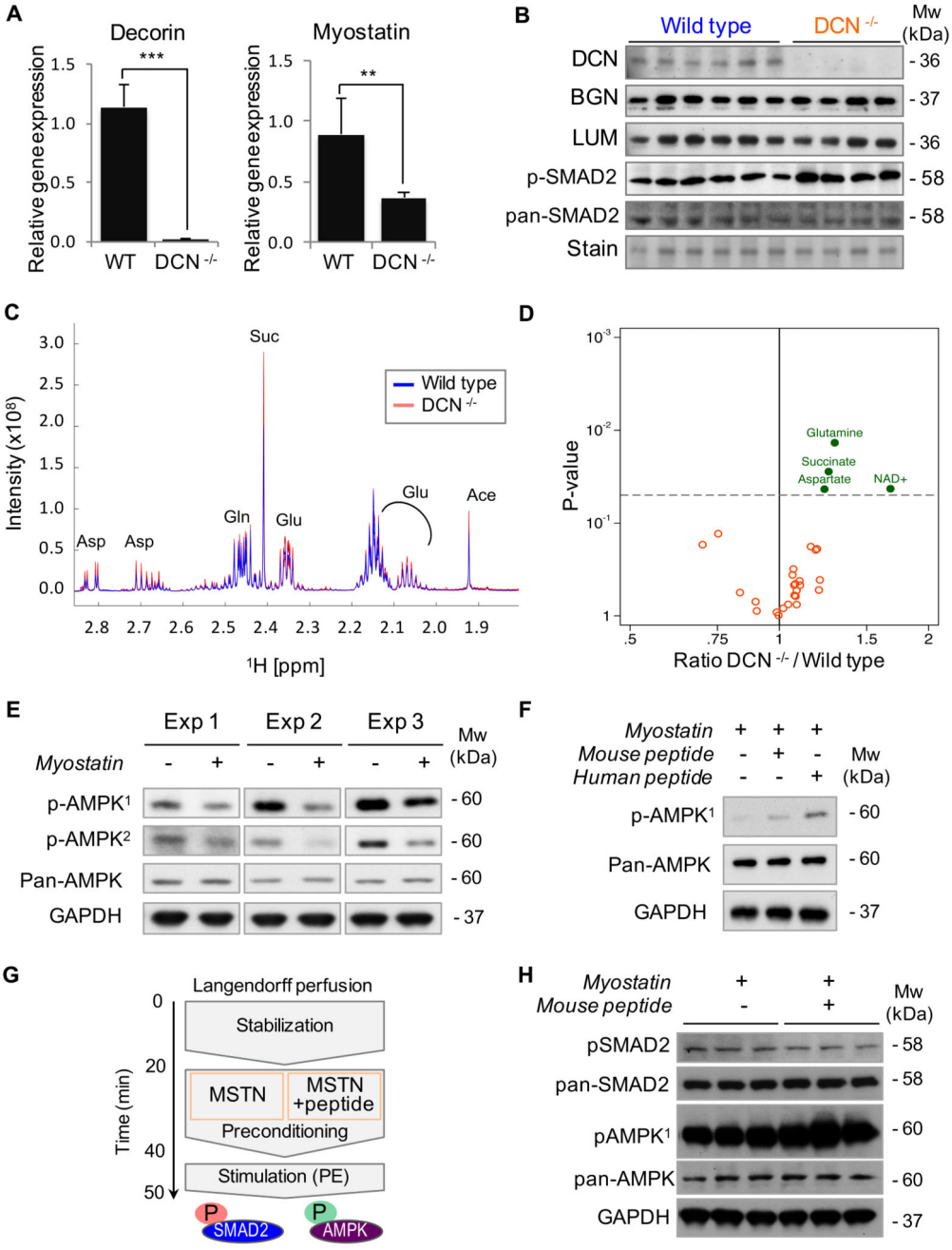

Figure 6. Effect of decorin on cardiac metabolism.

A) Deficiency of decorin was associated with reduced expression of myostatin in murine hearts. Bars represent mean ± SD. **B)** In hearts of decorin null mice, the abundance of closely related SLRPs, such as biglycan and lumican (LUM) was not affected, but phosphorylation of SMAD2 was increased. **C)** Overlay of $^{+}$H-NMR spectra from wild type and decorin null (DCN $^{-/-}$) hearts. **D)** Metabolic profiles of cardiac tissue from DCN $^{-/-}$ mice revealed elevated levels of glutamine (Gln), succinate (Suc), aspartate (Asp) and nicotinamide adenine dinucleotides (NAD^{+}, NADH). **E)** Myostatin represses AMPK

activation in rat cardiomyocytes. Immunoblotting was performed with two different antibodies for AMPK phospho-Thr_{172}. Levels of total AMPK (pan-AMPK) were unchanged. **F)** N-terminal decorin peptides from mouse or human origin (20μM) reversed the effect of myostatin on AMPK phosphorylation. Rat cardiomyocytes were stimulated with Iso and PE after incubation with myostatin for 2 hours. **G)** Schematic summary of the experiment in Langendorff perfused mouse hearts. **H)** Phosphorylation levels of AMPK and SMAD2 were used as readouts for inhibition of myostatin signaling by the N-terminal decorin peptide. **p<0.01; ***p<0.001.

Europe PMC Funders Author Manuscripts

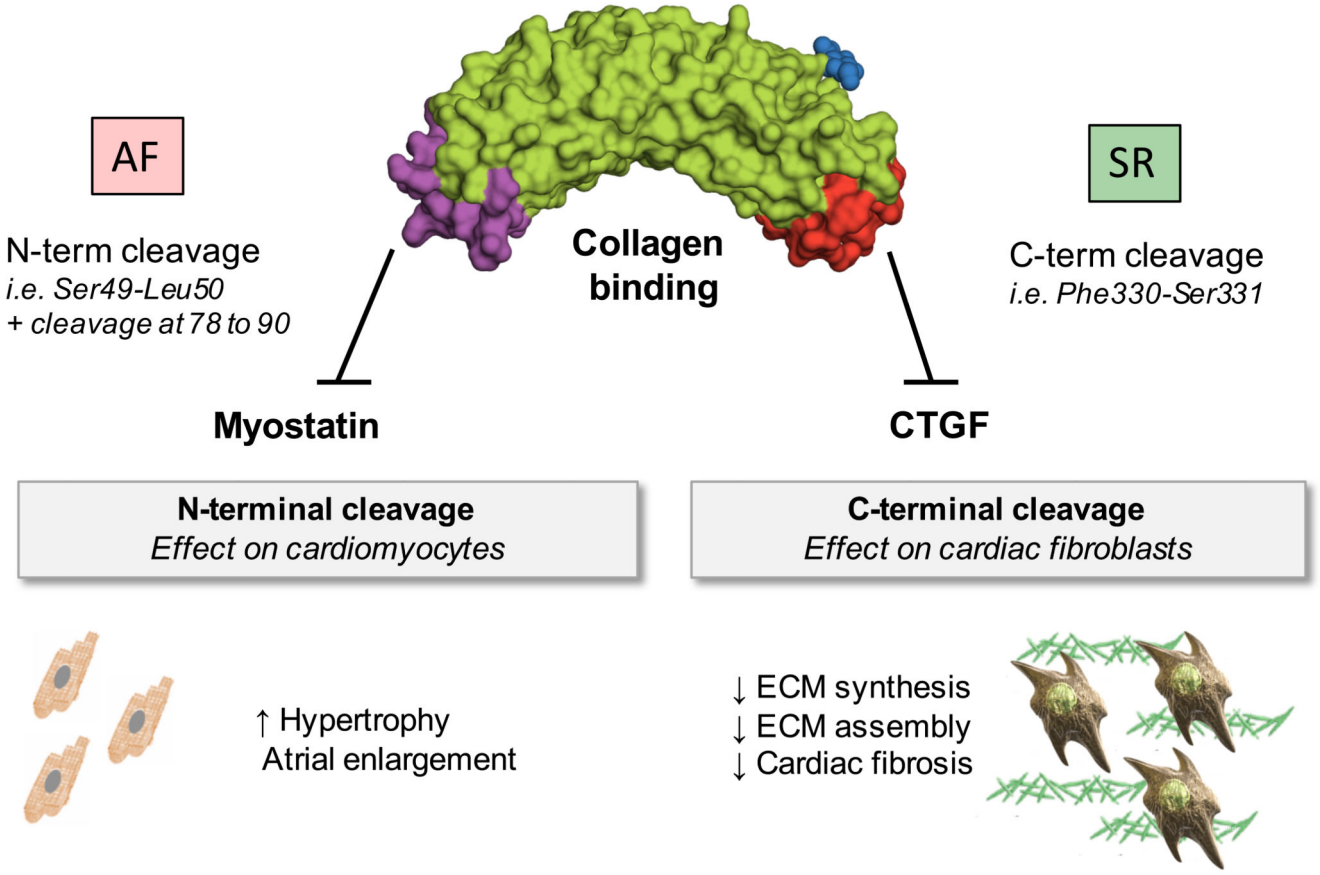

Figure 7. Decorin in human atria.

Decorin cleavage constitutes a mechanism for local regulation of growth factor bioactivity in the human cardiac ECM. N-terminal cleavage of decorin was observed in patients with persistent AF and gives rise to peptides with anti-myostatin activity. C-terminal truncation is more common in atria than ventricles and releases the CTGF-binding domain of decorin.

Europe PMC Funders Author Manuscripts

Europe PMC Funders Author Manuscripts

Table 1

Identification of ECM and ECM-Associated Proteins in Human Atrial Appendages

Proteins (97)	GuHCl (Input)	Glycoprotein Enrichment	Glycopeptide Analysis
Alpha-1-acid glycoprotein 1	+	+	
Alpha-1-acid glycoprotein 2		+	
Alpha-1B-glycoprotein	+	+	
Alpha-2-HS-glycoprotein		+	+
Annexin A2	+		
Apolipoprotein A-I	+		
Apolipoprotein A-IV	+		+
Apolipoprotein C-III	+		
Apolipoprotein E	+		
Asporin	+		
Basal cell adhesion molecule	+	+	+
Beta-2-glycoprotein 1	+	+	+
Biglycan	+		
Cadherin-13		+	
Cadherin-2	+	+	+
Cartilage intermediate layer protein 1		+	
Cartilage oligomeric matrix protein			+
Cathepsin G	+		
Chymase	+		
Clusterin	+	+	+
Collagen alpha-1(I)	+		
Collagen alpha-1(II)	+		
Collagen alpha-1(III)	+		
Collagen alpha-1(IV)	+		+
Collagen alpha-1(V)	+		
Collagen alpha-1(VI)	+		+
Collagen alpha-1(VIII)	+		
Collagen alpha-1(XV)	+		
Collagen alpha-1(XVIII)	+	+	
Collagen alpha-1(XXVIII)	+		+
Collagen alpha-2(I)	+		+
Collagen alpha-2(IV)	+		+
Collagen alpha-2(V)	+		
Collagen alpha-2(VI)	+		+
Collagen alpha-3(V)	+		
Collagen alpha-3(VI)	+	+	+
Collagen alpha-6(VI)		+	+
Decorin	+	+	+
Dermatopontin	+		

Proteins (97)	GuHCl (Input)	Glycoprotein Enrichment	Glycopeptide Analysis
Dystroglycan	+		+
Elastin	+		
EMILIN-1			+
Extracellular superoxide dismutase	+		
Fibrillin-1	+	+	
Fibromodulin	+		
Fibronectin	+	+	
Fibulin-2		+	+
Galectin-1	+		
Galectin-3	+		
Galectin-3-binding protein	+	+	
Glypican-1	+		
Hepatoma-derived growth factor		+	
Insulin-like growth factor-binding protein 7		+	
Intercellular adhesion molecule 1		+	
Kininogen-1		+	
Lactadherin	+		
Laminin subunit alpha-2	+		
Laminin subunit alpha-4	+		
Laminin subunit alpha-5	+		
Laminin subunit beta-1	+		
Laminin subunit beta-2	+	+	+
Laminin subunit gamma-1	+	+	
Latent-TGFβ-binding protein 2		+	
Latent-TGFβ-binding protein 4		+	
Leukocyte elastase inhibitor	+		
Lumican	+	+	+
Mast cell carboxypeptidase A	+		
Matrix Gla protein	+		
Matrix-remodeling-associated protein 7		+	
Metalloproteinase inhibitor 3	+		
Mimecan	+	+	+
Natriuretic peptide A	+		
Neural cell adhesion molecule 1		+	
Neural cell adhesion molecule L1	+	+	+
Neutrophil defensin 1	+		
Nidogen-1	+	+	+
Nidogen-2	+	+	
Periostin	+		
Perlecan	+	+	
Podocan			+
Proactivator polypeptide		+	

Europe PMC Funders Author Manuscripts

Proteins (97)	GuHCl (Input)	Glycoprotein Enrichment	Glycopeptide Analysis
Prolargin	+	+	+
Protein AMBP		+	
Proteoglycan 4		+	+
RPE-spondin		+	
Secreted frizzled-related protein 1	+		
Secreted phosphoprotein 24	+	+	
Serum amyloid P-component	+	+	+
Target of Nesh-SH3	+	+	
Tenascin		+	
Tenascin-X	+	+	+
TGFβ-induced protein ig-h3	+		
Tryptase beta-2	+		
Tubulointerstitial nephritis antigen-like	+	+	
Versican	+	+	+
Vitronectin	+	+	+
Zinc-alpha-2-glycoprotein		+	

+ denotes identification by one of the three proteomics strategies